Investigations for Chest Wall Deformities

6

Rajeev Shukla, Trupti Kolvekar, and Shyam K. Kolvekar

Abstract

Congenital chest wall deformities encompass a wide spectrum of conditions and present the patient with varying severities of cardiorespiratory and psychological dysfunction. Surgical intervention has been shown to alleviate symptoms and improve overall psychological wellbeing. Throughout history many different surgical correction techniques have been described for the treatment of congenital chest deformities. One factor that is common to all these surgical techniques is the necessity for detailed pre-operative workup. This chapter aims to explore the imaging modalities that can be used in the pre-operative evaluation of patients with a spectrum of congenital chest wall deformities.

Keywords

Pectus excavatum • Funnel chest • Haller Index • Nuss • Imaging • MRI • Chest x-ray • CMR • Sternal imaging • Jeune Syndrome • Asphyxiating thoracic dystrophy • Poland Syndrome • Sternal cleft

Introduction

Pectus excavatum (PE) is the most common congenital chest deformity. It is characterised by posterior depression of the sternum and adjacent costal cartilages, thereby reducing the antero-posterior distance of the thoracic cage [1, 2]. As many as 50 % of patients have a right sided dominant sternal depression [3]. Most patients present in their first year of life, but rarely do infants and young children exhibit clinical symptoms [4]. In adolescence patients may present

R. Shukla, MChem(Hons), MB, BS(Lon)
Department of Cardiothoracic Surgery, The Heart Hospital, University College London Hospital NHS Trust, London, UK

T. Kolvekar, BSc Biochemistry (Hon)
The Department of Structural Molecular Biology, University College London, London, UK

S.K. Kolvekar, MS, MCh, FRCS, FRCS (CTh) (✉)
Department of Cardiothoracic Surgery, University College London Hospitals, The Heart Hospital and Barts Heart Center, London, UK
e-mail: kolvekar@yahoo.com

S.K. Kolvekar, H.K. Pilegaard (eds.), *Chest Wall Deformities and Corrective Procedures*,
DOI 10.1007/978-3-319-23968-2_6

with cardiorespiratory symptoms, including exercise intolerance, fatigue, decreased stamina, exercise-induced wheezing [3, 4]. As many as 25 % of PE patients have increased incidence of respiratory tract infections or asthma and more than 50 % experience sharp pains in the lower anterior chest. Tachypnoea and palpitations are also common [3].

Moderate to severe deformities can result in significant displacement of the heart into the left chest resulting in considerable physiological impairment. Compression of the heart between the sternum and vertebral column was evident in early pathological studies [5] and thus explain some of the symptoms experienced by patients.

Throughout history many surgical correction techniques for PE have been described. One factor that is common to all these surgical techniques is the necessity for detailed pre-operative workup subsequent to patient selection for operative intervention [6]. This section explores the variety of imaging modalities that can be effectively utilised in evaluating the severity of PE and thus a means for quantifying the deformity.

Haller Index

Imaging for detailed anatomical assessment of PE deformity forms an essential component of preoperative workup and enables accurate quantification of the severity of sternal depression, the Haller Index [7].

The Haller Index was developed from CT scan analysis of a single image of the deepest part of the PE deformity. In their study Haller et al. calculated the ratio between the transverse diameter and the anteroposterior diameter, measured from the posterior surface of the sternum to the anterior surface of the vertebral body at the point of maximal depression. This was performed in 33 patients who underwent corrective surgery for PE deformity and compared with age-matched non-pectus controls. Haller found that all operated patients had a Haller Index of >3.25 (mean 4.42) and non-pectus controls <3.25 (mean 2.56) [8–11]. In adolescents and children, the Haller Index may range from 1.9 to 2.7 due to differences in chest wall configuration linked to age and gender. It was found that girls between ages 0–6 years and 12–18 years tended to have a higher Haller index than boys of the same age [12–15]. In clinical practice, it is widely accepted that a Haller Index >3.25 is indicative of a severe pectus deformity [16]. When combined with criteria obtained from adjunct tests including pulmonary function tests, cardiology evaluation to determine cardiovascular physiological impairment, a Haller Index >3.25 can be an indication for surgical correction [2, 8, 10, 11]. Various imaging modalities have been employed during the evaluation of pectus deformity with the aim to provide an accurate Haller Index and additional information regarding the effects on the local anatomy (Fig. 6.1) [2, 13, 14].

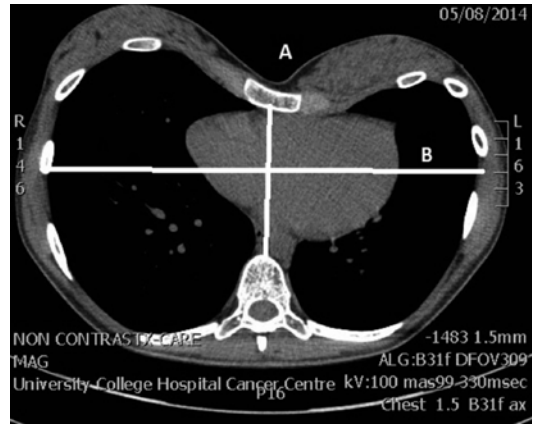

Fig. 6.1 Haller Index on CT scan

Chest X-ray

Evaluation of patients with plain radiographs is performed in two projections, frontal and lateral [15, 16]. PE deformity can produce characteristic findings of right middle lobe opacification on the frontal view that can often be mistaken for right middle lobe pneumonia or atelectasis [15]. This abnormal appearance is in fact due to compression of anterior chest wall soft tissue [15]. Other features that may also be apparent on frontal

Fig. 6.2 Chest x-ray PA view

projections include displacement of the cardiac silhouette to the left in more than 50 % of patients [17]. Takahashi et al. found obliteration of the descending aortic interface in 30 % of PE cases reviewed retrospectively in a cohort of 70 patients. Although no significant relationship was found between this and the severity of thoracic deformity, an indirect correlation to cardiac rotation angle does appear evident [18].

Lateral projections demonstrate posterior displacement of the sternum that is evident as an opacity filling the retrosternal space with ribs projecting anterior to the sternum, thus confirming PE deformity (Figs. 6.2, 6.3, 6.4, and 6.5) [15].

CT Scan

Computerised tomography (CT) scans have long been the primary imaging modality for evaluation of PE deformity. As described earlier, the Haller Index for objectively grading the severity of PE deformity was developed through the use of CT scans by dividing the transverse diameter of the chest by the anteroposterior diameter at the point of maximal sternal depression. In addition, CT scans can effectively demonstrate the degree of cardiac compression and displacement and its relationship to the sternum, the degree of pulmonary compression and atelectasis, asymmetry of the chest, sternal torsion and compensatory

Fig. 6.3 Chest x-ray with left lateral view

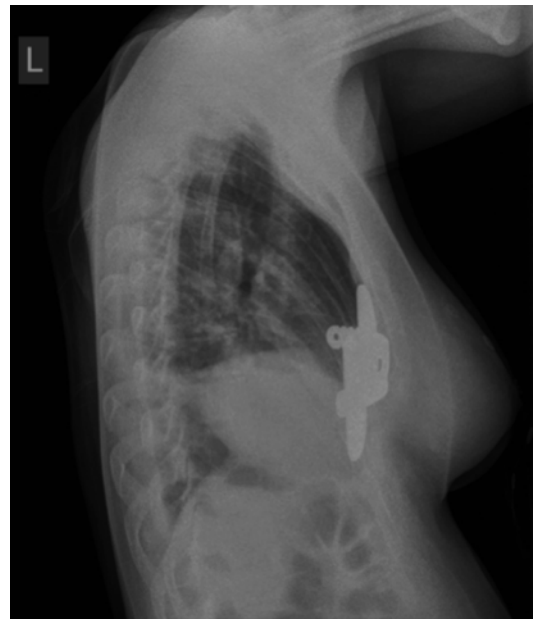

Fig. 6.4 Chest x-ray left lateral with the bar

development of a barrel chest (Figs. 6.6, 6.7, 6.8, 6.9, 6.10, and 6.11) [2, 19].

MRI and CMR

Certain centres have adopted Magnetic Resonance Imaging as the primary imaging modality to calculate the Haller Index. The primary advantage over CT is the absence of ionising radiation [10]. Piccolo et al. demonstrated strong comparability of Haller Indices and Asymmetry Indices obtained using fast MRI and CT scanning. In addition, fast MRI demonstrates excellent soft tissue contrast and thus high quality assessment of cardiac displacement or rotation, great vessel anomalies and asymmetric volume between left and right hemithorax (Fig. 6.12) [20, 21].

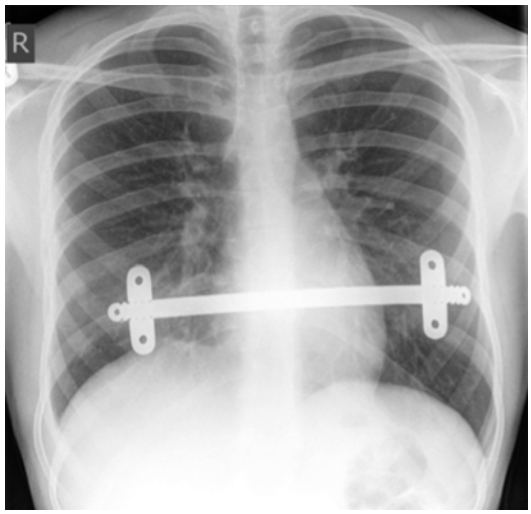

Fig. 6.5 Chest x-ray with the bar

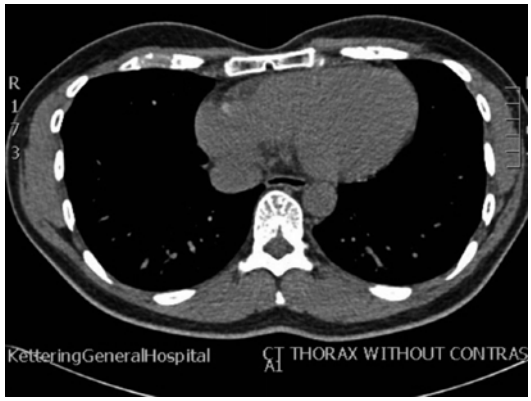

Fig. 6.6 CT scan with minimal depression and displacement

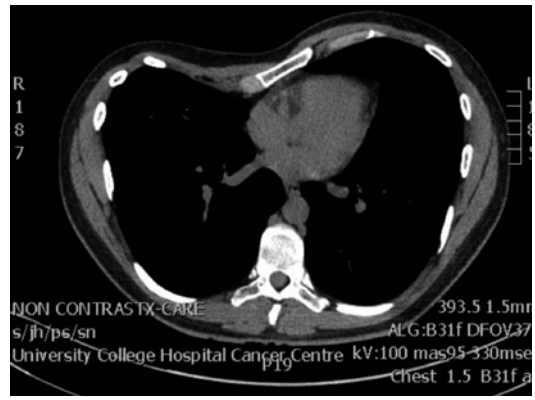

Fig. 6.7 CT scan with tilt of sternum with depressed right side

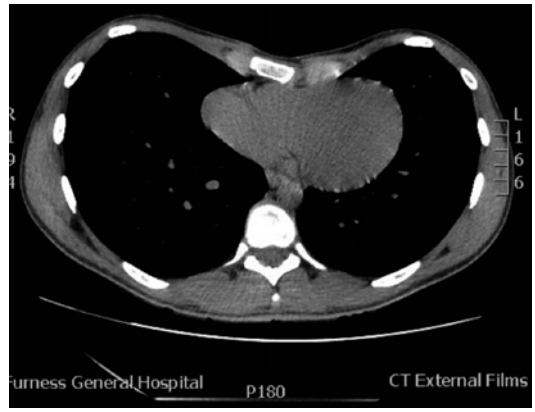

Fig. 6.8 CT scan with depression more on left side

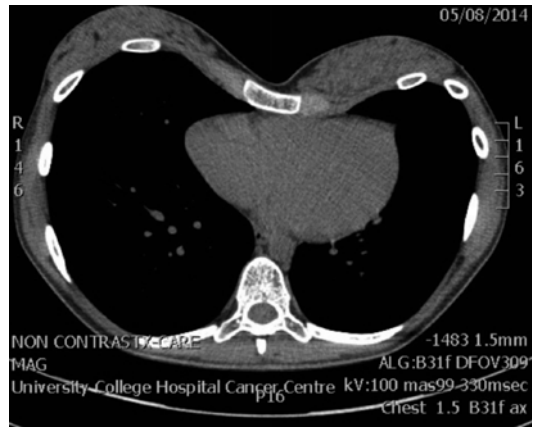

Fig. 6.9 CT scan with leftward tilt and depression

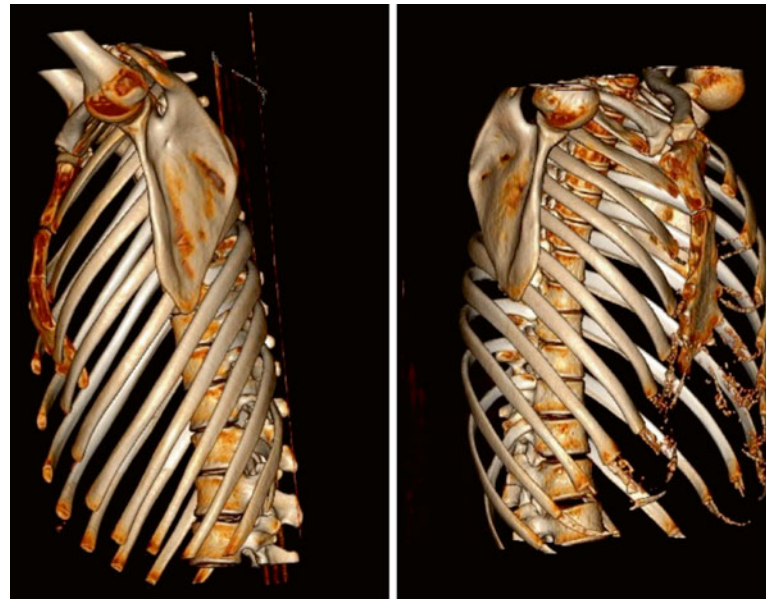

Fig. 6.10 3D reconstruction from CT showing the sternal depression and ribs alignment (**a**) lateral view; (**b**) oblique view

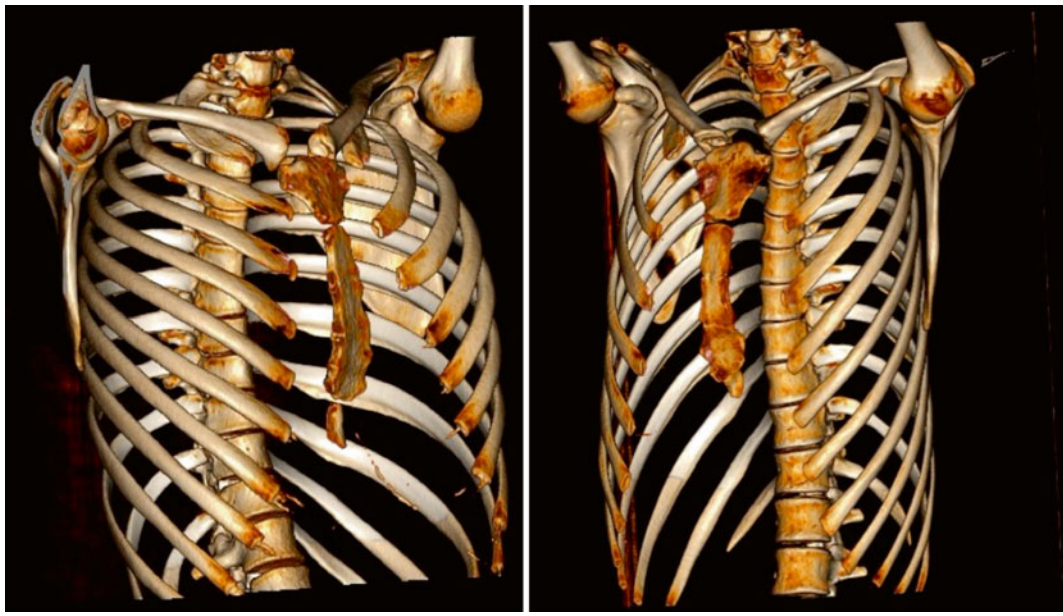

Fig. 6.11 3D reconstruction from CT showing the sternal depression and ribs alignment oblique view (**a**) right oblique view; (**b**) left oblique view

CMR has also been investigated as a potential imaging modality with the aim to delineate the anatomical and physiological components of pectus excavatum in addition to calculating the Haller Index. Saleh et al. demonstrated statistically significant higher HI in PE patients compared to non pectus patients (9.6 versus 2.8). The group were also able to demonstrate significant left lateral shift of the heart compared to controls (84 % versus 64 %) and reduction in right ventricular ejection fraction, which may be suggestive of changes in myocardial performance [22]. Humphries et al. have also demonstrated similar results with calculated HI of PE and non pectus patients [23].

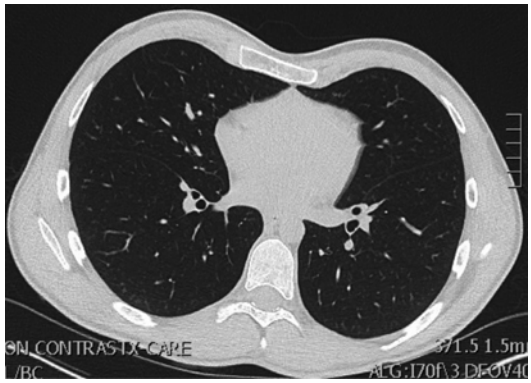

Fig. 6.12 MRI scan transverse section showing sternal depression

Echocardiography

Echocardiograms are performed to search for the presence of major valvular pathology and chamber compression (Fig. 6.13). The right ventricle and atrium can be compressed by the sternum resulting in problems during diastolic filling [20].

Mitral valve prolapse is seen in up to 17 % of patients with PE. Evaluation of the aortic root is also important particularly in patients who have been diagnosed with Marfans Syndrome [3, 7, 20].

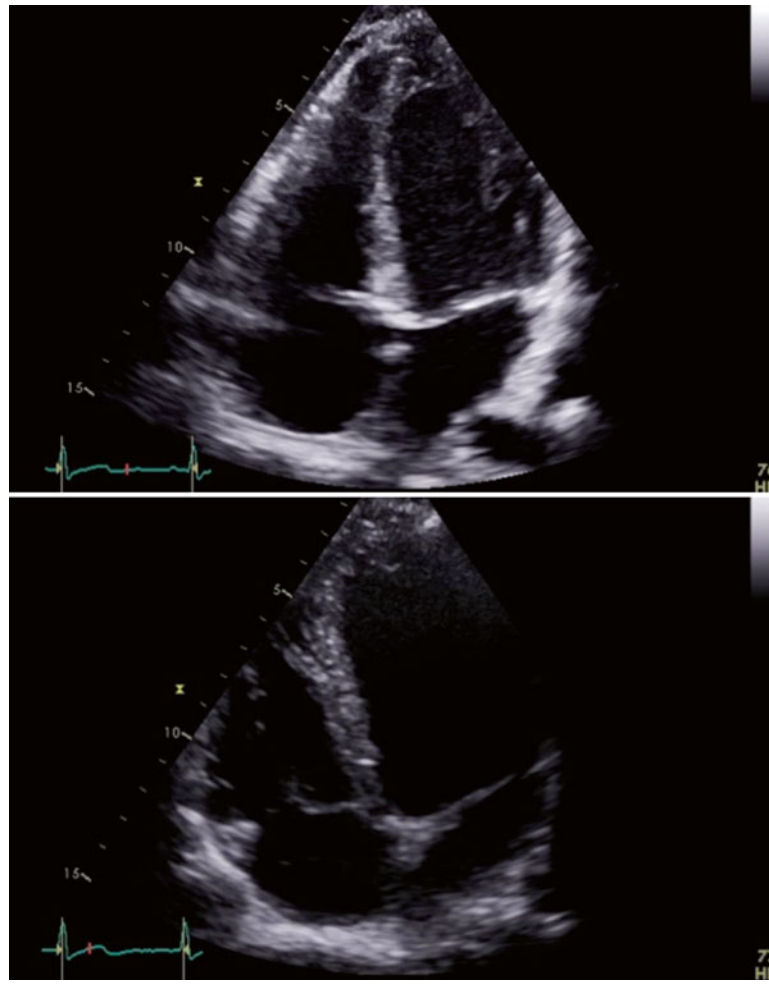

Fig. 6.13 Echocardiogram with four-channel view

Summary

Recent discussion has questioned the absolute necessity of performing a CT scan for evaluation of PE deformity. The main factor in searching for alternative imaging techniques is the high doses of radiation that are being delivered by CT scans to patients in their adolescence or younger who are being assessed for PE deformity. Four independent groups have evaluated the use of two-view chest x-rays in the pre-operative assessment of patients with PE deformity and conclude strong comparability of HI calculated from chest x-rays with that of CT scans and strong interobserver correlation. The unanimous recommendations from these studies is to replace CT imaging with chest X rays as the primary imaging modality for PE surgical workup, which would result in a 100 fold reduction in effective radiation dose [1, 24–26]. The counter argument to this is that chest x-rays provide no information regarding sternal asymmetry or torsion or the degree of cardiac compression and displacement [19]. One study concluded that no additional information was gleaned from a CT scan that was not already evident from two-view CXRs and instead adopted the use of low dose CT scanning comprising of five to seven slices through the point of maximal sternal depression in addition to two view CXRs. This has reduced radiation doses by up to 80 % [27] while still providing comprehensive visualisation of the local anatomy. In addition to significantly reducing the radiation exposure a substantial cost saving is also achievable when employing this strategy for pre-operative assessment [24].

Other groups have investigated the use of MRI and CMR scanning as the primary imaging modality and thus eliminating ionising radiation exposure completely. Two separate studies have shown favourable results for using MRI over CT scans to calculate the HI and AI while detailing anatomical information such as displacement, rotation or compression of the heart or great vessel anomalies [10, 21]. In addition to no radiation exposure the images can be acquired in less than 5 min without any compromise in quality. Further research demonstrates that cine MR can provide additional diagnostic information through evaluation of chest morphology and chest wall kinetics [10]. CMR has also been shown to be beneficial for the same reasons as MRI but also in its ability to provide accurate and dynamic assessment of cardiovascular function and thus potentially eliminating the need for echocardiographic studies.

It is clear that a growing number of institutions are moving away from the use of full chest CT scanning as the primary modality for calculating HI and AI in patients with PE deformity and adopting imaging strategies that have lower or no radiation exposure. All of the studies performed with alternative imaging modalities to CT have a smaller cohort of patients but so far the results are encouraging.

Pectus Carinatum

Pectus carinatum (PC) is the second most common anterior chest wall anomaly occurring in approximately one in 1500 live births with a male to female ratio of 4:1 [20, 28]. It is characterised by sternal and costal cartilage elevation [20] and depending on the area involved can be classified into two variant types [20, 28].

Chondrogladiolar subtype is the more common deformity involving protrusion of the mid to lower portion of the anterior chest wall and inferior costal cartliages and part of the gladiolus [28, 29]. Chondromanubrial deformity or Currarino-Silverman syndrome in cases with associated congenital heart disease, is the less common subtype involving protrusion of the second and third costal cartilages with elevation of the sternomanubrial joint [20, 28].

Pre-treatment radiological evaluation of PC aims to establish the presence of an increased antero-posterior (AP) diameter in association with protrusion of the sternum [28]. Features that may be apparent on plain chest radiography

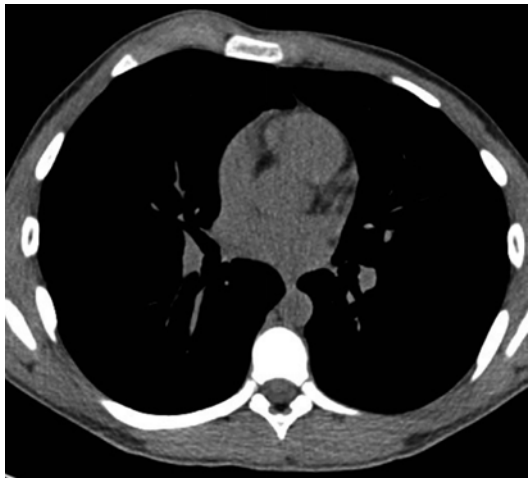

Fig. 6.14 Uneven shape

include a narrowed thorax and scoliosis on posteroanterior projections. Lateral projections provide a more striking image of the deformity. Features that can be identified include the presence of a bowed, short, comma-shaped sternum with an increased AP diameter [28]. Further differentiation of PC into its variant forms, as determined by the site of sternal protrusion, can also be adequately demonstrated on lateral projections as shown by various groups [28–31]. Computed tomography (CT) has also been advocated for use in the evaluation of patients with PC as part of the routine pre-treatment assessment (Fig. 6.14) [20]. Desmaris et al. conclude that CT scanning should be reserved for cases with 'mixed' deformities, where sternal angle measurements can be easily calculated [30]. More recently Lee et al. presented their experience with the use of MRI for evaluation of PC. Early results show MRI to be highly effective at measuring sternal angle rotation and asymmetry index in PC patients, which can be used in pre-treatment evaluations [32].

Poland Syndrome

Poland syndrome (PS) is an uncommon chondrocostal anomaly occurring in approximately 1 in 30,000 live births [33, 34]. It is characterised by

Fig. 6.15 CT scan with left sided hypoplasia

the absence or hypoplasia of the costosternal part of the pectoralis major and minor muscle and absent costal cartilages or ribs 2, 3 and 4 or 3, 4 and 5 [33–35]. PS is essentially a unilateral defect and may be associated with lung herniation. Two-thirds of cases involve the right side [34, 35]. Surgical intervention in PS is reconstructive to protect organs, which are at risk of damage due to bony defects and cosmetic to fill the defect resulting from absent pectoralis muscles [20]. The primary imaging modalities used in pre-operative assessment include chest radiography and computed tomography (CT) (Fig. 6.15) [20, 33]. Unilateral hyperlucency mimicking radical mastectomy is often seen in chest radiography [33]. However, for detailed assessment of the extent of muscular, rib and costal cartilage involvement a combined imaging using CT and MRI has been advocated, with CT providing a clearer depiction of bony defects and the absence of the pectoralis minor muscle and MRI providing better tissue contrast [36]. CT scan with 3D reconstruction allows for greater anatomical detail thereby enhancing surgical planning [20, 36, 37].

Sternal Cleft

A sternal cleft is a rare abnormality, which is classified as partial or complete. Partial defects can be located superiorly or inferiorly. Complete defects arise as a result of complete lack of fusion of the sternum in the midline [28, 34].

CT is considered to be the imaging modality of choice as it depicts midline defects clearly and when reformatted can delineate between complete and incomplete defects [28]. Successful prenatal diagnosis of sternal clefts using 3D and 4D sonography have been reported by various groups [6, 38, 39]. Pasoglou et al. [39] reported a multimodality approach to imaging of sternal cleft using CT, MRI and US. The latter investigations can be used prenataly without exposing the foetus to radiation. However, images obtained by US can be affected by maternal obesity [40]. CT is recommended for use in the neonatal period to safely exclude the presence of associated skeletal abnormalities [39].

Jeune Syndrome

Jeune syndrome [asphyxiating thoracic dystrophy (ATD)] is a rare autosomal recessive genetic disorder causing skeletal dysplasia [41, 42]. It is characterised by a small, narrow thoracic cage and variable limb shortness [41, 43]. Radiographic findings are specific enough to enable easy distinction from other skeletal dysplasias except the Ellis-van Crevald syndrome [41, 44]. Typical findings include a narrow, bell-shaped thorax with short, horizontal orientation of ribs and irregular costochondral junctions, elevated clavicles, short iliac bones with a typical trident appearance of the acetabula, relatively short and wide long bones of the extremeties and hypoplastic phalanges of both hands and feet with cone-shaped epiphyses [41, 42]. Various groups report the value of performing prenatal sonography in diagnosing a foetus with severe forms of ATD. The important findings suggestive of a diagnosis of ATD included severe shortened ribs, thorax, short limbs without polydactyl [45–47].

References

1. Wu T-H, et al. Usefulness of chest images for the assessment of pectus excavatum before and after a Nuss repair in adults. Eur J Cardiothorac Surg. 2013;43:283–7.
2. Frantz FW. Indications and guidelines for pectus excavatum repair. Curr Opin Pediatr. 2011;23:486–91.
3. Fonkalsrud EW. Current management of pectus excavatum. World J Surg. 2003;27:502–8.
4. Sawar ZU, DeFlorio R, O'Connor SC. Pectus excavatum: current imaging techniques and opportunities for dose reduction. Semin Ultrasound CT MR. 2014;35(4):374–81.
5. Malek MH, et al. Cardiovascular function following surgical repair of pectus excavatum – a metaanalysis. Chest. 2006;130:506–16.
6. Brochhausen C, et al. Pectus excavatum: history, hypotheses and treatment options. Interact Cardiovasc Thorac Surg. 2012;14:801–6.
7. Jaroszewski D, Notrica D, McMahon L, Steidley ED, Deschamps C. Current management of pectus excavatum: a review and update of therapy and treatment recommendations. J Am Board Fam Med. 2010;23:230–9.
8. Haller AJ, Kramer SS, Lietman SA. Use of CT scans in selection of patients for pectus excavatum surgery: a preliminary report. J Pediatr Surg. 1987;22(10):904–6.
9. Rebeis EB, et al. Anthropometric index for quantitative assessment of pectus excavatum. J Bras Pneumol. 2004;30(6):501–7.
10. Marcovici PA, LoSasso BE, Kruk P, Dwek JR. MRI for the evaluation of pectus excavatum. Pediatr Radiol. 2011;41:757–8.
11. Blanco FC, Elliott ST, Sandler AD. Chest wall reconstruction. Semin Plast Surg. 2011;25:107–16.
12. Eich GF, Kellenberg CJ, Willi UV. Radiology of the chest wall. Paediatric chest imaging: chest imaging in infants and children. Springer, Berlin. 2013; p. 315–6.
13. Nuss D, Kelly RE. Indications and technique of Nuss procedure for pectus excavatum. Thorac Surg Clin. 2010;20:583–97.
14. Kelly RE. Pectus excavatum: historical background, pre-operative evaluation and criteria for operation. Semin Pediatr Surg. 2008;17(3):181–93.
15. Robbins LP. Pectus excavatum. Radiol Case Rep (online). 2011;6:460.
16. Baez JC, Lee EY, Restrepo R, Eisenberg RL. Chest wall lesions in children. AJR Am J Roentgenol. 2013;200:W402–19.
17. Morshuis WJ, et al. Chest radiography in pectus excavatum: recognition of pectus excavatum-related signs and assessment of severity before and after surgical correction. Eur Radiol. 1994;4(3):197–202.
18. Takahashi K, Sugimoto H, Ohsawa T. Obliteration of the descending aortic interface in pectus excavatum: correlation with clockwise rotation of the heart. Radiology. 1992;182(3):825–8.
19. Goretsky MJ, Kelly RE, Croitoru D, Nuss D. Chest wall anomalies: pectus excavatum and pectus carinatum. Adolesc Med. 2004;15:455–71.
20. Colombani P. Preoperative assessment of chest wall deformities. Semin Thorac Cardiovasc Surg. 2009;21:58–63.
21. Piccolo RL, et al. Chest fast MRI: an imaging alternative on pre-operative evaluation of pectus excavatum. J Pediatr Surg. 2012;47:485–9.

22. Saleh RS, et al. Cardiovascular magnetic resonance in patients with pectus excavatum compared with normal controls. J Cardiovasc Magn Reson. 2010;12:73. 1–10.
23. Humprhies CM, Anderson JL, Flores JH, Doty JR. Cardiac magnetic resonance imaging for perioperative evaluation of sternal eversion for pectus excavatum. Eur J Cardiothorac Surg. 2013;43:1110–3.
24. Poston PM, et al. Defining the role of chest radiography in determining candidacy for pectus excavatum repair. Innovations. 2014;9(2):117–21.
25. Khanna G, Jaju A, Don S, Keys T, Hildebolt CF. Comparison of Haller Index values calculated with chest radiographs versus CT for pectus excavatum evaluation. Pediatr Radiol. 2010;40:1763–7.
26. Mueller C, Saint-Vil D, Bouchard S. Chest x-ray as a primary modality for preoperative imaging of pectus excavatum. J Pediatr Surg. 2008;43:71–3.
27. Rattan AS, Laor T, Ryckman FC, Brody AS. Pectus excavatum imaging: enough but not too much. Pediatr Radiol. 2010;40:168–72.
28. Restrepo CS, et al. Imaging appearances of the sternum and sternoclavicular joints. Radiographics. 2009;29:839–59.
29. Shamberger RC, Welch KJ. Surgical correction of pectus carinatum. J Pediatr Surg. 1987;22(1):48–53.
30. Desmaris TJ, Keller M. Pectus carinatum. Curr Opin Pediatr. 2013;25(3):375–81.
31. Grissom LE, Harcke HT. Thoracic deformities and the growing lung. Semin Roentgenol. 1998;33(2):199–208.
32. Lee R, et al. MRI evaluation of pectus carinatum: preliminary experience. European Congress of Radiology. Scientific Exhibit Poster, Vienna C-0022; 2015.
33. Jeung MY, et al. Imaging of chest wall disorders. Radiographics. 1999;19:617–37.
34. Torre et al. Chest wall deformities: an overview on classification and surgical options, chap. 8. In: Topics in thoracic surgery. InTech, Europe. 2012. p. 117–36.
35. Urschel Jr HC. Poland syndrome. Semin Thorac Cardiovasc Surg. 2009;21(1):89–94.
36. Ribeiro RC, et al. Clinical and radiographic poland syndrome classification: a proposal. Aesthet Surg J. 2009;29(6):494–504.
37. Cingel V, et al. Poland syndrome: from embryological basis to plastic surgery. Surg Radiol Anat. 2013;35(8):639–46.
38. Izquierdo MT, Bahamonde A, Domene J. Prenatal diagnosis of a complete cleft sternum with 3-dimensional sonography. J Ultrasound Med. 2009;28:379–83.
39. Pasoglou V, et al. Sternal cleft: prenatal multimodality imaging. Pediatr Radiol. 2012;42:1014–6.
40. Twomey EL, et al. Prenatal ultrasonography and neonatal imaging of complete cleft sternum: a case report. Ultrasound Obstet Gynecol. 2005;25:599–601.
41. Thakkar PA, Aiyer S, Shah B. Asphyxiating thoracic dystrophy (Jeune syndrome). J Case Rep. 2012;2(1):15–7.
42. de Vries J, et al. Jeune syndrome: description of 13 cases and a proposal for follow-up protocol. Eur J Pediatr. 2010;169(1):77–88.
43. Shaheen R, et al. A founder CEP120 mutation in Jeune asphyxiating thoracic dystrophy expands the role of centriolar proteins in skeletal ciliopathies. Hum Mol Genet. 2015;24(5):1410–9.
44. Oberklaid F, et al. Asphyxiating thoracic dysplasia. Clinical, radiological and pathological information on 10 patients. Arch Dis Child. 1977;52(10):758–65.
45. Tongsong T, et al. Prenatal sonographic findings associated with asphyxiating thoracic dystrophy (Jeune syndrome). J Ultrasound Med. 1999;18:573–6.
46. Hollander NS, et al. Early prenatal sonographic diagnosis and follow-up of Jeune syndrome. Ultrasound Obstet Gynecol. 2001;18:378–83.
47. Schinzel A, et al. Prenatal sonographic diagnosis of Jeune syndrome. Radiology. 1985;154(3):777–8.